Experimental Investigations of a Modified Taylor-Couette Flow

A. Esmael, A. El Shrif

Abstract—In this study the instability problem of a modified Taylor-Couette flow between two vertical coaxial cylinders of radius R_1, R_2 is considered. The modification is based on the wavy shape of the inner cylinder surface, where inner cylinders with different surface amplitude and wavelength are used. The study aims to discover the effect of the inner surface geometry on the instability phenomenon that undergoes Taylor-Couette flow. The study reveals that the transition processes depends strongly on the amplitude and wavelength of the inner cylinder surface and resulting in flow instabilities that are strongly different from that encountered in the case of the classical Taylor-Couette flow.

Keywords— Hydrodynamic Instability, Modified Taylor-Couette Flow, Turbulence, Taylor vortices.

I. INTRODUCTION

FLOW instabilities affect many industrial and engineering applications that involve fluid flow phenomenon. The understandings of physical mechanisms that lead to such instabilities are of great interest. Taylor Couette flow problem was one of the most flow configurations studied to understand the hydrodynamic instability phenomenon. It gives a simple and clear flow configuration that involves many instability stages which ends by a turbulent flow regime [1]. But there are still several issues to be addressed such as the effect of flow geometry on these instabilities. Applying a little geometrical modification on this flow can lead to flow behaviors that are completely different from the transition procedures that undergoes a classical Taylor-Couette flow. The modified Taylor-Couette consists of two coaxial cylinders of which the outer cylinder is smooth and fixed and the inner cylinder is rotating and has a wavy surface with a specified amplitude and wavelength. Such flow configuration has been studied by [2], where they have used measuring techniques based on the particle imaging velocimetry (PIV) and shear force on the wall to localize transition stages and study the interaction between Taylor vortex and that imposed by the inner cylinder surface geometry. The radial and axial velocity components strongly influence the generation of vortices. They depend on the axial position, amplitude, and wavelength of the wavy surface. By increasing the rotational speed of the inner cylinder, the flow becomes unstable at a certain critical point. This instability is manifested in the form of a generation of additional vortex cells induced by the inner cylinder surface

A. Esmael is a lecturer at Fuculty of Engineering, Almergib University, Alkhoms, Libya (corresponding author phone: +218 92 502 7432; e-mail: esrtah@yahoo.com).

A. El Shrif is a lecturer at Fuculty of Engineering, Almergib University, Alkhoms, Libya (e-mail: aelshrif@ gmail.com).

geometry. As rotational speed increases beyond some critical velocity, the flow bifurcate [3] (Hopf bifurcation) to an asymmetric solution where each vortex pair is formed by two vortex of different size, in which the large vortex becoming larger, up to 1.5 times the size of small vortex, which can be explained by the presence of an azimuthal wave of axial pressure that affects the whole flow [4].

In this study the hydrodynamic instability problem of Taylor–Couette flow using a wavy shape inner cylinder surface has been considered. The study will explain the effect of inner cylinder surface shape on the flow behavior during instability stages that undergoes this flow configuration. Also it will permit more understanding to the mechanisms that led to the described instability stages.

II. EXPERIMENTAL APPARATUS

The experimental apparatus used is the same as that used by [5], where it consists of two coaxial cylinders. A transparent outer cylinder of Plexiglass with radius $R = 65.3\,mm$, thickness of $5mm$ and height $H = 287mm$ is used. Inner coaxial rotating cylinder is fitted inside the outer cylinder. The geometry of the different wavy surface inner cylinders are given in the Table I, where a is the amplitude, λ is the wavelength, K is the wave number and

$$d = R_2 - \left(R_{1,max} + R_{1,min}\right)/2$$

TABLE I
GEOMETRY OF THE INNER CYLINDER

Cyl	Rmax	Rmin	Rm	a	λ	K	d
C_1	55,20	47,39	51,30	3,91	35,88	8	14
C_2	59,12	43,52	51,30	7,83	35,88	8	14
C_3	55,20	47,39	51,30	3,91	71,75	4	14
C_4	59,12	43,52	51,30	7,83	71,75	4	14

The entire device is mounted vertically on two Plexiglass plates of $25mm$ thickness and a dimension of $(250 \times 250)\ mm^2$. Therefore a removable enclosure lid containing an O-ring sealing is added with a necessary bearing for the centering and guiding of the inner cylinder. The fluid used in the experiments is an aqueous solution of PLuracol (EMCAROX, ICI product). The fluid exhibits temperature-dependent Newtonian fluid characteristics in the range of the experiments. The axial velocity profile has been measured using a Pulsed emission Ultrasound Velocity meter. The UVP

device measures the axial velocity component in 128 points distributed along the measuring window.

III. ANALYSIS OF THE RESULTS

Four cases have been studied as shown in Table I depending on the geometry of the wavy inner cylinder surface. The first case C_1 corresponds to an inner cylinder surface with short wavelength and low amplitude, C_2 corresponds to an inner cylinder surface with short wavelength and big amplitude, C_3 corresponds to an inner cylinder surface with a long wavelength and low amplitude and C_4 uses an inner cylinder with long wavelength and big amplitude. The forgoing instability analysis will be based on the study of flow behavior for each case in the range of Taylor number begins from $Ta \approx 50$ to $Ta \approx 600$. The evolution of velocity fields as well as the spectral analysis of the flows will be discussed in details.
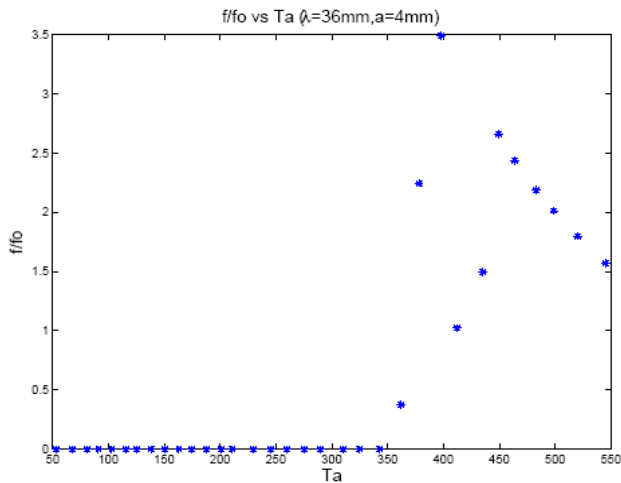

Fig. 1 Evolution of the frequency ratio (f/f_o) vs. Ta case C_1

Case C_1

At low Taylor numbers the flow is stable and there is no main frequency in the Spectral diagram Fig. 1. The first transition is located at Ta =370, where the main frequency drops rapidly above the value f_o. It must be noted that in this case, the spectral diagram exhibits random perturbations which are much greater than that appeared in the case of smooth cylinder [5]. At this Taylor number the wavelength does not change and remains the same as that imposed by the geometry of the inner cylinder surface. The analysis of the axial velocity field show a steady flow at Ta=53. The contours of the axial velocity profile Fig. 2 show a difference between the relative instability of source and sink zones within the flow where sink zones appear to be more disturbed compared to the sources zones. At Ta=174 the flow becomes disturbed over time and the axial flow velocity become five times greater. Velocity contours show an amplification of the difference between the sizes of the source and sink zones. By increasing Taylor number to Ta=529, the axial velocity becomes twice its

value in the previous case. The positive and negative cells are now asymmetrical. Small and large Taylor cells appear clearly in this stage Fig. 3 and here also sink zones appear to be more perturbed in time than the source zones.
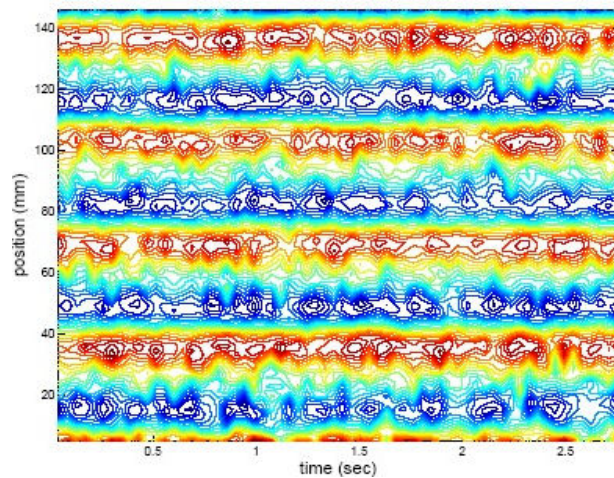

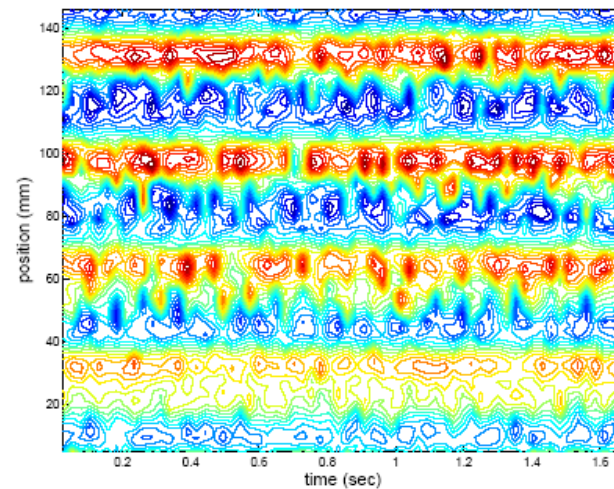Fig. 2 Contours of axial velocity profile at Ta = 53, case C_1

Fig. 3 Contours of axial velocity profile at Ta = 529

Case C_2

As shown by Fig. 4, the flow does not exhibit any main frequency in the period $Ta < 242$. As Taylor number increases beyond this limit the flow oscillates at a relative frequency f/f_o < 1. For $325 < Ta < 463$ the flow becomes steady with two asymmetric Taylor cells per cylinder wavelength. Beyond $Ta > 463$, the flow has a spectrum of decreasing frequency which begins to increase again beyond $Ta > 530$. The analysis of the axial velocity profile shows a stable flow with no perturbations. By increasing Taylor number beyond 276, azimutal waves superimpose on the Taylor cells and the velocity become 5 times greater. For Ta=377 Fig. 5 the flow passes by a Hopf bifurcation [3] and continues in steady state. The velocity contours make evident the change in size of the

213

Taylor cells, where one of them becomes larger than the other. As Taylor number increases beyond Ta = 571 the flow goes to a modulated oscillatory state with source zones that are more stable in time than the sink zones.

Fig. 4 Evolution of the frequency ratio (*f/f$_o$)* vs. Ta case C_2
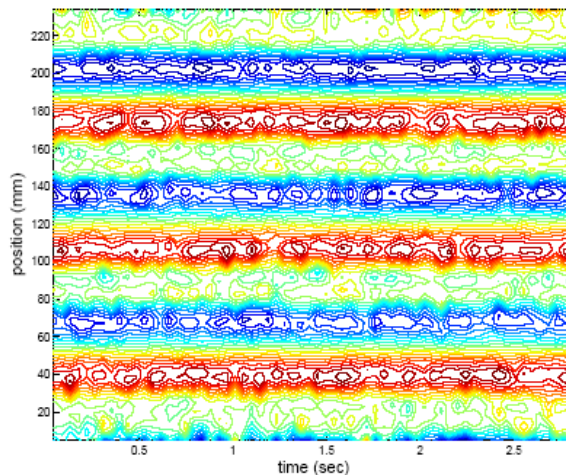

Fig. 5 Contours of axial velocity profile at Ta = 377

Case C_3

The flow in this case is very different from the previous cases where it contains initially 4 cells per wavelength. At Ta=160 the flow oscillates at frequency ratio (*f/f$_o$ =0.9)* with azimuthal waves which superimpose on the Taylor cells. Then immediately after, the flow becomes stable with two Taylor cells per wavelength. Beyond Ta=370 the flow transits back from the steady state to an oscillatory state of low frequency. This behavior appears clearly in the Fig. 6, where the wavelength presents an intermittent behavior varying from two Taylor vortices to four vortexes per wavelength and vice versa. Note that among the four vortices there are two inner vortices rotating in the same direction as the cylinder geometric vortex and the other two rotate in the opposite

directions Fig. 7. At Ta=157 the flow becomes wavy with the appearance of azimuthal waves, but it does not stay long time. By increasing Taylor number the flow transits to chaotic states with two incommensurate frequencies, where one can clearly see the doubling of vortices in the axial velocity profile.
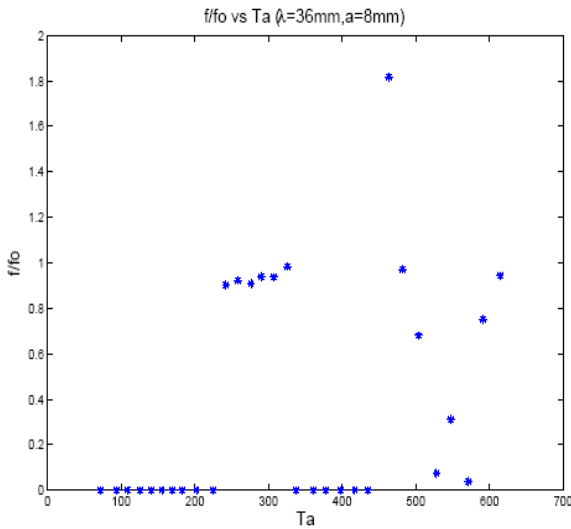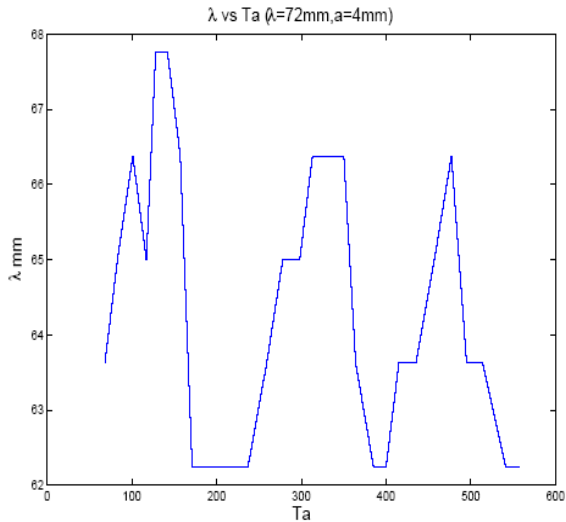
Fig. 6 Evolution of the wave length vs. Ta case C_3

Fig. 7 Contours of axial velocity profile at Ta = 83

Case C_4 :

The flow in this case shows a stable velocity profile at Ta=77 with two Taylor vortex cells per wave length Fig. 8. At Ta=165 the flow becomes unstable and transits to an oscillatory state with two deformed vortex for each wave length. At moderate Taylor number the flow exhibits a stable flat velocity profile with two cells per wavelength and is characterized also by the presence of a small perturbation between each vortex pair Fig. 9. As Taylor number becomes greater than Ta=444 the spectrum of the flow present a new behavior which differs from the preceding cases where three

high frequencies appear Fig. 10. At large Taylor number (Ta= 584) the flow transits to a clearly disordered state Fig. 11.

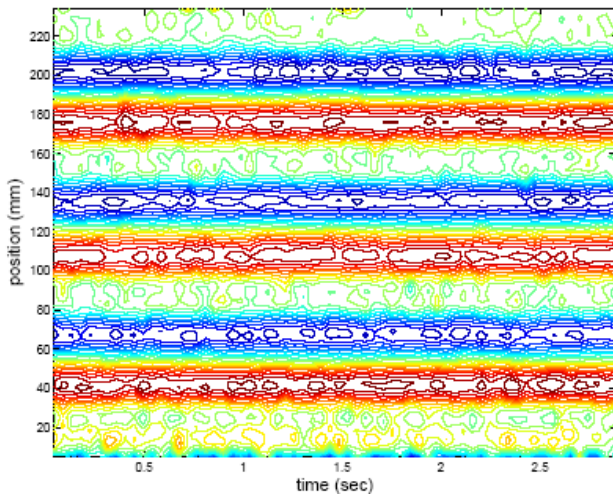mainly concern the small vortex cells (sink zones) which likely disappear.
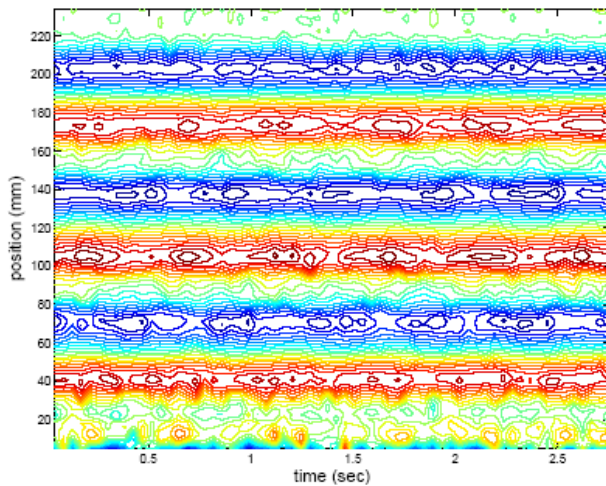

Fig. 8 Contours of axial velocity profile at Ta = 77

Fig. 10 Evolution of the frequency ratio (f/f_o) vs. Ta case C_4

Fig. 9 Contours of axial velocity profile at Ta = 356

Fig. 11 Contours of axial velocity profile at Ta = 584

IV. CONCLUSION

As it clear from the results, the different flow regimes and transitions depend strongly on the length and amplitude of the wavy inner cylinder surface. The main contribution of this work is the analysis of the axial velocity fields in space and time using the ultrasonic approach. This analysis allowed during different transition stages to follow the evolution of the frequency and wavelength of the flow. The direct exploitation of the axial velocity profile permitted to specify clearly the topology and in particular the number and size of vortex cells and the relative stability of source and sink zones of the flow. Indeed, when there are oscillations in the flow, source zones appear to be less stable over time than sink zones. When the flow structure switches from vortex arrangement of 4 cells / λ to 2 cells / λ in the case C_3 , the oscillations of the flow
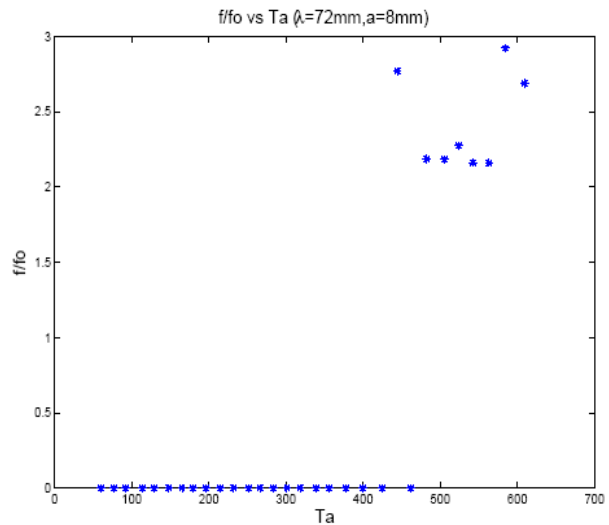
REFERENCES

[1] Dong S., "Direct Numerical Simulation of Turbulent Tyaylor-Couette Flow", J. Fluid Mech. (2007), vol. 587, pp. 373–393.
[2] Rafique M., "Etude de l'écoulement entre deux cylindres coaxiaux à entrefer constant et à entrefer ondule par la surface du cylindre intérieur tournant", Doctorat de INPL, 1999.
[3] M. Rafique, S. Skali Lami. "A study of steady state flow in modified Taylor-Couette system: Inner rotating wavy cylinder coaxial with a smooth stationary outer cylinder". 11th International Couette-Taylor Workshop, Germany, 1999, 105-106.
[4] Drozdov S. M., Skali Lami S., Rafique M., "An asymmetrical periodic vortical structures and appearance of the self-induced pressure gradient in the modified Taylor Flow", 13th Int. Taylor Couette Workshop, 2003.
[5] Esmael A., Elshrif A., "Experimental Investigations of Classical Taylor Couette Flow", Third Tunisian conference on mechanics, Sousse Mars 2014.